THE UNIVERSITY *of* EDINBURGH

Edinburgh Research Explorer

Neighbor network in a polydisperse hard-disk fluid: Degree distribution and assortativity

OPEN ACCESS

Neighbor network in a polydisperse hard-disk fluid: Degree distribution and assortativity

Alexandros Chremos and Philip J. Camp*

School of Chemistry, University of Edinburgh, West Mains Road, Edinburgh EH9 3JJ, United Kingdom
(Received 5 April 2007; published 13 November 2007)

The neighbor network in a two-dimensional polydisperse hard-disk fluid with diameter distribution $p(\sigma) \sim \sigma^{-4}$ is examined using constant-pressure Monte Carlo simulations. Graphs are constructed from vertices (disks) with edges (links) connecting each vertex to k neighboring vertices defined by a radical tessellation. At packing fractions in the range $0.24 \leq \eta \leq 0.36$, the decay of the network degree distribution is observed to be consistent with the power law $k^{-\gamma}$ where the exponent lies in the range $5.6 \leq \gamma \leq 6.0$. Comparisons with the predictions of a maximum-entropy theory suggest that this apparent power-law behavior is not the asymptotic one and that $p_k \sim k^{-4}$ in the limit $k \to \infty$. This is consistent with the simple idea that for large disks, the number of neighbors is proportional to the disk diameter. A power-law decay of the network degree distribution is one of the characteristics of a scale-free network. The assortativity of the network is measured and is found to be positive, meaning that vertices of equal degree are connected more often than in a random network. Finally, the equation of state is determined and compared with the prediction from a scaled-particle theory. Very good agreement between simulation and theory is demonstrated.

I. INTRODUCTION

For over four decades the science of complex networks was based on results for random graphs, obtained by Erdös and Rényi in 1959 [1]. Recent analyses reveal that the topologies of most large, real networks deviate from those of random networks [2]. Examples of real networks include the World Wide Web [3,4], the Internet [5], metabolic systems and protein-protein interactions [6–8], sexual contacts [9], collaborations between scientists [10] and between movie actors [11], and scoring totals of Brazilian football players [12]. The most significant deviations from random-network behavior appear in the tail of the *degree distribution p_k*, which is the probability of a given vertex possessing connections to k other vertices. In random networks p_k is Poissonian, while p_k for many real networks varies asymptotically like $k^{-\gamma}$, where γ is a positive exponent [11]. In qualitative terms, a *scale-free* network is characterized by a small number of highly connected vertices called "hubs"; for a general introduction, see Ref. [13]. Many authors identify scale-free networks as those possessing power-law degree distributions but as discussed fully in Ref. [14], this is a necessary but not sufficient condition. In what follows, we will be largely concerned with power-law degree distributions and the term "scale free" will be employed, but it should be borne in mind that, strictly speaking, other properties are required for the network to be termed scale free [14].

It has been suggested—but not yet confirmed—that growth and preferential attachment are possible mechanisms by which real-world, scale-free networks can emerge [2]; the addition of nodes to networks may capture the intrinsic evolutionary behavior of some real-world examples. Dynamical models of the growth of cellular networks—including the effects of cell division and disappearance—can also give rise to scale-free neighbor networks [15,16]. Stochastic models

have been proposed and studied which can successfully reproduce certain features of real networks [11,17]; however, there are some features which cannot yet be reproduced. An example is the assortativity of a network [18], which measures the extent to which vertices with equal degree link with one another: in assortative networks, vertices with equal degree are linked to one another more frequently than in a random network; in disassortative networks, vertices with equal degree are linked to one another less frequently than in a random network. To quote Newman, "An interesting observation is that essentially all social networks measured appear to be assortative, but other types of networks (information networks, technological networks, biological networks) appear to be disassortative. It is not clear what the explanation for this result is, or even if there is any one single explanation. (Probably there is not.)" [19]. Nonetheless, it has been shown that assortativity and clustering (which means more linked vertices share a common neighbor than would be expected by chance) can arise if social networks are divided in to distinct groups or communities [20].

Scale-free networks are rare in real and model condensed-matter systems. One important example is the scale-free contact network in the Apollonian packing of circles [21], in which the circle diameter distribution decays according to a power law with an exponent of about 1.3 [22]. The mechanical, percolation, and conductive properties of materials possessing Apollonian-packing networks have been shown to exhibit unusual dependences on the number of vertices [21]. Such models may describe the distribution of force in granular materials such as concrete and networks of voids in porous media. The percolation properties of such networks [21,23] will clearly be of relevance to the characteristics of certain porous media. Apollonian packing has also been identified as a model for networks of connected minima on potential-energy surfaces of atomic clusters [24]; the transition states (edges) between minima (vertices) exhibit a scale-free distribution [25–27].

This article is concerned with the possibility of generating a simple scale-free network in molecular simulations of a

*philip.camp@ed.ac.uk

simple fluid. The model consists of polydisperse hard disks in two dimensions, in which the distribution of disk diameters (σ) varies asymptotically like $\sigma^{-\alpha}$, where α is a positive exponent. The equilibrium structure of the fluid phase is determined using Monte Carlo (MC) simulations, conducted at constant pressure (strictly tension). Naively one might expect the number of neighbors of a given disk to be proportional to the circumference and hence σ. Due to the broad distribution of particle diameters, neighbors are identified using the radical tessellation [28] proposed as a suitable alternative to the Voronoï construction which is usually applied to one-component systems. If the tail of the diameter distribution follows a power law, then perhaps the neighbor distribution will vary in a similar way. Identifying particles with vertices, and the separation vectors between neighboring disks as edges, this situation could give rise to a scale-free neighbor network, with the large particles playing the role of the hubs. In this article it is shown that (i) there are indications that the neighbor network in the polydisperse hard-disk fluid possesses a power-law degree distribution, which is one of the properties of a scale-free network, and (ii) the neighbor network is highly assortative; i.e., vertices with equal degree are directly connected more often than in a random network. This is an interesting situation, because the equilibrium properties of the fluid are static, and hence dynamic mechanisms of scale-free network formation—e.g., preferential attachment—are not applicable.

Polydisperse hard-disk fluids are of considerable intrinsic interest, for example, as models of colloidal monolayers, froths and foams, and packing and segregation in granular materials. The packing of binary mixtures of hard disks has been studied extensively and is shown to be highly nontrivial [29–31]; for instance, the distributions of neighbors and of cell area (as obtained from radical tessellations) show distinct contributions arising separately from the small and large disks, indicating the clustering of disks with equal size. Fluids with more than two components have received far less attention, although it has been noted than in some respects the statistics of the radical tessellations may conform to those of a random tessellation [29]. Specifically, it has been found that fluids of disks with a linear, decreasing diameter distribution obey the Aboav-Weaire law, which states that the average total number of sides of the cells (determined by tessellation) neighboring a cell with k sides increases linearly with k [32–34]. It has been shown that the Aboav-Weaire law is a consequence of a maximum-entropy (ME) principle [35,36], the argument being that it can be written as a linear superposition of two basic constraints, these being that $\Sigma_k p_k = 1$ and for a two-dimensional (2D) tessellation $\Sigma_k k p_k = 6$ (Euler); therefore, the Aboav-Weaire law provides no new constraints and so it leads to the ME distribution. It might therefore be anticipated that in the polydisperse hard-disk fluid considered in this work, a maximum-entropy distribution may provide an adequate description of the nearest-neighbor network measured in simulations.

From the viewpoint of liquid-state physics, it is interesting to construct expressions for the equations of state of highly polydisperse fluids. In statistical mechanical terms, this may stimulate progress in understanding dense, complex fluids, such as the mixtures of macromolecules found inside
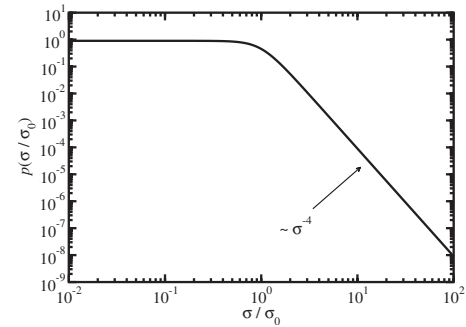

FIG. 1. Normalized disk-diameter distribution $p(\sigma) = C/[1+(\sigma/\sigma_0)^4]$ plotted on a log-log scale to highlight the asymptotic σ^{-4} behavior.

living cells [37]. Therefore, a simple equation of state is derived using scaled-particle theory (SPT) [38] and compared with (essentially exact) results from MC simulations.

This article is organized as follows. Section II details the hard-disk model, summarizes the MC and SPT approaches to be employed, and presents the derivation of a ME estimate of p_k. The results are reported and discussed in Sec. III, and Sec. IV concludes the paper.

II. MODEL AND METHODS

The model consists of N hard disks confined to a square cell of area A. The disk-diameter distribution is given by

$$p(\sigma) = \frac{C}{1+(\sigma/\sigma_0)^\alpha}, \qquad (1)$$

where $\sigma \geq 0$, σ_0 is a reference diameter, α is a positive exponent, and C is the normalization constant. This particular choice of distribution was chosen so that there is a finite number of small particles (important for the simulations) and because it rapidly approaches the asymptotic form $p(\sigma) \sim \sigma^{-\alpha}$. The value of α should be small enough to give a long tail to the distribution, but large enough such that the first few moments are well defined. The second moment is required to exist so that one can define a packing fraction, given by $\eta = \pi \rho \langle \sigma^2 \rangle / 4$, where the angular brackets denote an average over $p(\sigma)$ and $\rho = N/A$ is the number density. The second moment is finite only for $\alpha > 3$, so the present work is focused on the distribution with $\alpha = 4$, the normalization constant and first two moments of which are

$$C = \frac{2\sqrt{2}}{\pi \sigma_0}, \qquad (2)$$

$$\langle \sigma \rangle = \frac{\sigma_0}{\sqrt{2}}, \qquad (3)$$

$$\langle \sigma^2 \rangle = \sigma_0^2. \qquad (4)$$

$p(\sigma)$ is plotted in Fig. 1 on a log-log scale to show the crossover to a power-law decay for $\sigma \gtrsim \sigma_0$.

A. Monte Carlo simulations

Constant-temperature, constant-pressure MC simulations of $N=10^4$ polydisperse hard disks were performed in a square cell with periodic conditions applied [39]. The hard-disk system is athermal, and so the reduced pressure employed in the simulations is defined as $P^*=P\sigma_0^2/k_BT$, where k_B is Boltzmann's constant and T is the temperature. Ten different simulation configurations were used, each consisting of particles with diameters drawn randomly from $p(\sigma)$. Results obtained with the ten configurations at a given reduced pressure were averaged.

On average, one MC cycle consisted of N attempted displacements of randomly selected disks, N_A trial displacements of $\ln A$ [39], and one cluster move, the latter implemented using Dress and Krauth's cluster algorithm [40] with reflection rather than rotation [41]. The cluster moves are vital for equilibration, because the displacements of large disks are severely hampered by the large number of neighboring small disks. In a few words, each cluster move begins with the selection of a random pivot point within the simulation box. A disk is chosen at random and is subjected to a point reflection about the pivot. Any disks that overlap with the reflected disk are themselves reflected, and this process is repeated until there are no more overlaps. This algorithm works particularly well at low to intermediate densities, but it fails at high densities due to all of the particles being part of the same "cluster" [41]. For each state point the equilibration phase consisted of about 10^5 MC cycles with $N_A=1-20$, depending on the pressure. Production runs consisted of a further 10^5 MC cycles. At intervals of 10 MC cycles, radical tessellations [28] were computed and the network statistics were incremented. In the standard 2D Voronoï construction, the edges of the tessellation are perpendicular bisectors of the lines joining the centers of neighboring disks. When neighboring disks are of very different size, the bisectors may intersect with the larger disks. In the radical tessellation, this problem is avoided by forming edges with the loci of points from which the lengths of the tangents to neighboring disks are equal.

B. Scaled particle theory

The derivation of a simple equation of state from SPT [38] is now summarized. To begin, the excess chemical potential (in units of $k_BT=\beta^{-1}$) of a scaled disk with diameter $\lambda\sigma$ is given in the limit of small λ by the Widom insertion formula [42]

$$\beta\mu^{\text{ex}}(\lambda\sigma) \approx -\ln\left[1 - \rho\int p(\sigma')v(\lambda\sigma,\sigma')d\sigma'\right], \quad (5)$$

where $v(\lambda\sigma,\sigma')$ is the excluded "volume" of two hard disks with diameters $\lambda\sigma$ and σ':

$$v(\lambda\sigma,\sigma') = \frac{\pi}{4}(\lambda\sigma+\sigma')^2. \quad (6)$$

The combination of Eqs. (5) and (6) can be expanded about $\lambda=0$ up to a linear term. An additional λ^2 term is chosen to yield the correct limit when $\lambda\rightarrow\infty$; in the case of a scaled

disk with area $\pi\lambda^2\sigma^2/4$, the reversible work of expanding the particle against the macroscopic pressure is $\pi P\lambda^2\sigma^2/4$. The result of these manipulations is an approximation to the excess chemical potential at fixed density and temperature:

$$\beta\mu^{\text{ex}}(\lambda\sigma) \simeq -\ln(1-\eta) + \frac{\pi\rho\sigma\langle\sigma'\rangle}{2(1-\eta)}\lambda + \frac{\pi}{4}\beta P\sigma^2\lambda^2. \quad (7)$$

To obtain an equation of state, appeal is made to a relation for hard particles derived by Smith and Labík [43,44]. Consider the quantity Y defined by the derivative of $\beta\mu^{\text{ex}}$ with respect to λ at $\lambda=1$, averaged over the diameter distribution of the inserted particle:

$$Y = \int p(\sigma) \left.\frac{d\beta\mu^{\text{ex}}(\sigma)}{d\lambda}\right|_{\lambda=1} d\sigma. \quad (8)$$

In microscopic terms, this derivative is related to the infinitesimal work of expanding a full-sized particle against the surrounding fluid. This is given by [45]

$$Y = \rho \int p(\sigma)p(\sigma')g(\sigma,\sigma') \left.\frac{\partial v(\lambda\sigma,\sigma')}{\partial\lambda}\right|_{\lambda=1} d\sigma\,d\sigma'$$

$$= \frac{1}{2}\pi\rho \int p(\sigma)p(\sigma')g(\sigma,\sigma')\sigma(\sigma+\sigma')d\sigma\,d\sigma', \quad (9)$$

where $g(\sigma,\sigma')$ is the partial pair correlation function for particles with diameters σ and σ', at contact. The right-hand side of this equation is simply related to the compressibility factor, $Z=\beta P/\rho$, which is easily obtained from the virial equation [46]

$$Z = 1 + \frac{1}{8}\pi\rho \int\int p(\sigma)p(\sigma')g(\sigma,\sigma')(\sigma+\sigma')^2 d\sigma\,d\sigma'. \quad (10)$$

Comparing Eqs. (9) and (10) leads to the simple relationship

$$Y = 2(Z-1). \quad (11)$$

This is the two-dimensional version of a result derived by Smith and Labík in Ref. [44]. Inserting the SPT result for $\beta\mu^{\text{ex}}(\lambda\sigma)$ [Eq. (7)] into Eq. (8) yields

$$Y = \frac{2\eta s}{(1-\eta)} + 2Z\eta, \quad (12)$$

where the packing fraction $\eta=\pi\rho\langle\sigma^2\rangle/4$ and $s=\langle\sigma\rangle^2/\langle\sigma^2\rangle$. Equating Eqs. (11) and (12) furnishes the final expression for the compressibility factor

$$Z = \frac{1+(s-1)\eta}{(1-\eta)^2}. \quad (13)$$

The expansion of Eq. (13) to first order in ρ is

$$Z = 1 + \frac{\pi}{4}(1+s)\langle\sigma^2\rangle\rho + \cdots, \quad (14)$$

which yields the correct second-virial coefficient (equal to half of the average excluded volume)

$$B_2 = \frac{1}{2} \int \int p(\sigma)p(\sigma')\frac{\pi}{4}(\sigma+\sigma')^2 d\sigma\,d\sigma' = \frac{\pi}{4}(1+s)\langle\sigma^2\rangle.$$

$$\text{(15)}$$

For the disk-diameter distribution in Eq. (1) with $\alpha=4$, $s=\frac{1}{2}$ and $Z=(1-\eta/2)/(1-\eta)^2=1+3\eta/2+\cdots$. Note that for the monodisperse hard-disk fluid, $s=1$ and the familiar SPT result $Z=1/(1-\eta)^2$ is recovered.

C. Degree distribution from maximum-entropy theory

We derive a simple, ME estimate of $p_k(\sigma)$, this being the joint probability distribution of neighbors for a disk with given diameter σ. The overall degree distribution p_k is then obtained by integration of $p_k(\sigma)$. The derivation relies on there being constraints on the mean and mean-square number of neighbors for a disk with given diameter. A very small disk is essentially an ideal point particle, and because such small disks are so numerous, the neighbor network will be essentially random with moments that will not depend sensitively on σ. (The degree distribution for Voronoï tessellations of random sets of points in a plane—the 2D Poisson-Voronoï tessellation—is known [47,48].) On the other hand, a very large disk is expected to have an average number of neighbors which scales linearly with σ. We make the following ansatz: the average number of neighbors for a disk with diameter σ is

$$K_1(\sigma) \equiv \frac{\sum_k kp_k(\sigma)}{p(\sigma)} = a_1 + b_1 f(\sigma),$$

$$\text{(16)}$$

where we have used the fact that $\Sigma_k p_k(\sigma)=p(\sigma)$ and the sums are restricted to $k \geq 3$ because triangles are the smallest polygons in the tessellation. a_1 and b_1 are parameters, and $f(\sigma)$ is a function with the properties $f(0)=0$ and $\lim_{\sigma\to\infty}[f(\sigma)\sigma_0/\sigma]=1$. Given the form of $p(\sigma)$, an obvious choice for $f(\sigma)$ is

$$f(\sigma) = \frac{(\sigma/\sigma_0)^{\alpha+1}}{1+(\sigma/\sigma_0)^\alpha}.$$

$$\text{(17)}$$

The mean-square number of neighbors, $K_2(\sigma) = \Sigma_k k^2 p_k(\sigma)/p(\sigma)$, is assumed to be such that the width of the distribution for a given σ is constant:

$$\frac{K_2(\sigma) - K_1^2(\sigma)}{K_1^2(\sigma)} = a_2.$$

$$\text{(18)}$$

The parameters a_1, b_1, and a_2 are then chosen so that

$$\int p(\sigma)K_1(\sigma)d\sigma = \langle k \rangle,$$

$$\text{(19)}$$

$$\int p(\sigma)K_2(\sigma)d\sigma = \langle k^2 \rangle,$$

$$\text{(20)}$$

where $\langle k \rangle=6$ (Euler) and $\langle k^2 \rangle$ are the averages for the whole network, and $\langle k^2 \rangle$ is to be taken from simulation. This leads to the relationships

$$b_1 = \frac{\langle k \rangle - a_1}{\langle f(\sigma) \rangle},$$

$$\text{(21)}$$

$$a_2 = \frac{\langle k^2 \rangle}{a_1^2 + 2a_1 b_1 \langle f(\sigma) \rangle + b_1^2 \langle f^2(\sigma) \rangle} - 1,$$

$$\text{(22)}$$

where a_1 will be retained as an adjustable parameter. The quantity $K_1(0)=a_1$ should be less than 6 because the average of $K_1(\sigma)$ over the whole diameter distribution—including the large disks—should be precisely 6. For the present diameter distribution (1) with $\alpha=4$, $\langle f(\sigma) \rangle=1/(2\sqrt{2})$ and $\langle f^2(\sigma) \rangle=21/32$. We now seek a ME solution for $p_k(\sigma)$ subject to the following constraints:

$$\sum_k p_k(\sigma) = p(\sigma),$$

$$\text{(23)}$$

$$\sum_k kp_k(\sigma) = p(\sigma)K_1(\sigma),$$

$$\text{(24)}$$

$$\sum_k k^2 p_k(\sigma) = p(\sigma)K_2(\sigma).$$

$$\text{(25)}$$

Maximizing the entropy $S=-\Sigma_{k\geq 3}p_k(\sigma)\ln p_k(\sigma)$ with respect to $p_k(\sigma)$ (with the method of Lagrange multipliers) leads to the result

$$p_k(\sigma) = \exp[\Lambda_0(\sigma) + \Lambda_1(\sigma)k + \Lambda_2(\sigma)k^2],$$

$$\text{(26)}$$

where the $\Lambda_i(\sigma)$s are adjusted to satisfy the constraints (23)–(25). Finally, p_k is obtained from the relation

$$p_k = \int p_k(\sigma)d\sigma.$$

$$\text{(27)}$$

III. RESULTS

A. Equation of state

Reliable simulation results were obtained for pressures up to $P^*=2$, corresponding to a packing fraction $\eta\simeq 0.45$. For higher pressures the cluster moves were seen to result in point reflections of increasingly large clusters, which ultimately precludes effective equilibration of the system. Presumably there is no crystallization at very high pressure. The equation of state—plotted as P^* versus η—for the polydisperse hard-disk fluid is shown in Fig. 2. The raw data are given in Table I. The SPT (13) and virial-expansion (14) results are shown for comparison. The SPT is surprisingly good, being accurate for packing fractions up to about 0.3.

B. Radical tessellation and degree distribution

Simulation snapshots at $P^*=1$ are shown in Fig. 3; the packing fraction at this pressure is $\eta\simeq 0.36$. For clarity, only a subdomain (containing 1600 particles) of a particular configuration is shown. Three different views are displayed: (a) the actual hard-disk configuration, (b) the radical tessellation, and (c) the Delaunay triangles formed by the links between neighboring vertices (defined by disks that share cell edges).
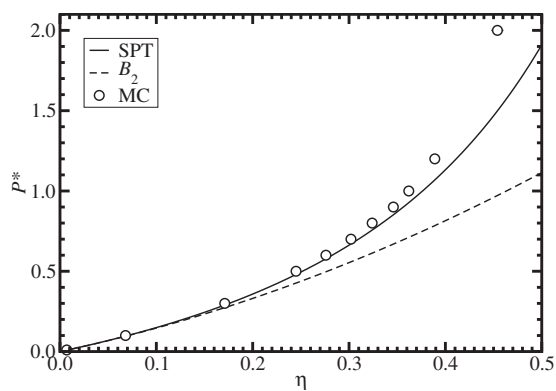
FIG. 2. Equation of state and reduced pressure $P^* = \beta P \sigma_0^2$ versus packing fraction η: MC simulations (points), SPT (solid line), and virial expansion with B_2 (dashed line).

FIG. 3. (Color online) Subdomain ($N=1600$ particles) of a simulation configuration at $P^*=1$ and $\eta \simeq 0.36$: (a) the actual hard-disk configuration, (b) the radical tessellation, and (c) the Delaunay triangles formed by the links between neighboring vertices.

On the basis of the radical tessellations, the degree distribution p_k was constructed, being the probability that a disk has k neighboring disks. Given that ten configurations were simulated, each containing 10^4 particles, the lower limit on p_k accessible from our simulations is $\sim 10^{-5}$. In all cases it was confirmed that the average number of links, $\langle k \rangle$, is precisely equal to 6. Figure 4 shows p_k as measured and averaged from simulations at $P^*=0.01$, 0.1, 0.5, 1, 1.2, and 2. Error bars on p_k represent the statistical uncertainty in the mean obtained from averaging over the ten distinct configurations. The small-k portions of p_k ($k \lesssim 10$) show only small variations over the entire range of pressures simulated. At low pressures ($P^* < 0.5$), p_k shows no sign of a long tail. At such low packing fractions, the particle positions are uncorrelated and the degree distribution resembles that of the 2D Poisson-Voronoï tessellation [47,48]. At pressures in the range $0.5 \leq P^* \leq 1$ it was observed that the tail of p_k for $k \gtrsim 21$ appears as a straight line on a log-log plot, indicating consistency with the power-law decay $k^{-\gamma}$. At higher pressures, no power-law tail is apparent over the range of k accessible in simulations. For all pressures $P^* \geq 0.1$, a kink is
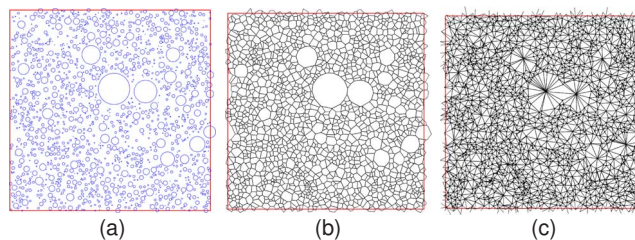
apparent in p_k at the point where $p_k \simeq 10^{-4}$. Since the proportions of particles contributing to p_k before and after the kink appear constant, this suggests that p_k is partitioned into "small-particle" and "large-particle" contributions, the latter possibly corresponding to an asymptotic scale-free regime.

Figure 5 shows the tails of p_k as measured in simulations with pressures in the range $0.5 \leq P^* \leq 1$. The kinks at $p_k \simeq 10^{-4}$ are more clearly visible. The asymptotic decay of p_k is consistent with a power law, but it is far from being unambiguous. It is difficult to access larger values of k because of limitations on the number of particles that can be simulated; this restricts the form of the diameter distribution and, in particular, necessitates the regularization of the distribution at $\sigma < \sigma_0$. Nevertheless, least-squares fitting of power laws to the tails of p_k yields the lines shown in Fig. 5. The corresponding fitting ranges and exponents (γ) are reported in Table I.

It has been pointed out that the least-squares fitting procedure may give rise to biased, and hence erroneous, results for the power-law exponent (γ) due to large fluctuations in the tail of the distribution [49,50]. There is an alternative fitting scheme based on a maximum likelihood estimator (MLE), which for power laws yields a simple, closed-form expression for the exponent [49,50]. We implemented this scheme on the cumulative probability $c_k = \Sigma_k^\infty p_k \sim k^{-\gamma+1}$,

TABLE I. Results from MC simulations of the polydisperse hard-disk fluid with $\alpha=4$: packing fraction η; mean and mean-square degree, $\langle k \rangle$ and $\langle k^2 \rangle$; relative width of the degree distribution, $w = \sqrt{\langle k^2 \rangle / \langle k \rangle^2 - 1}$; power-law exponent γ for the tail of p_k (and the range over which power-law behavior is observed) from least-squares (LS) fitting and a maximum likelihood estimator (MLE) [49,50]; assortativity r. Figures in parentheses are statistical uncertainties in the last digits based on one standard deviation.

| P^*	η	$\langle k \rangle$	$\langle k^2 \rangle$	w	γ (LS)	γ (MLE)	Range	r
0.01	0.0078(2)	6.00	37.758(4)	0.2210				0.475(8)
0.1	0.068(1)	6.00	37.78(7)	0.2220				0.472(14)
0.3	0.171(2)	6.00	37.88(3)	0.2285				0.467(10)
0.5	0.245(3)	6.00	38.18(3)	0.2445	6.0(1)	5.7	$21 \leq k \leq 28$	0.456(9)
0.6	0.276(3)	6.00	38.33(4)	0.2525	5.8(1)	5.7	$22 \leq k \leq 29$	0.448(7)
0.7	0.302(3)	6.00	38.44(4)	0.2581	5.9(1)	5.6	$23 \leq k \leq 31$	0.441(7)
0.8	0.324(3)	6.00	38.55(5)	0.2641	5.7(1)	5.5	$23 \leq k \leq 32$	0.433(7)
0.9	0.346(3)	6.00	38.67(4)	0.2698	5.6(1)	5.4	$24 \leq k \leq 33$	0.424(7)
1	0.362(2)	6.00	38.76(4)	0.2744	5.6(1)	5.4	$24 \leq k \leq 34$	0.420(6)
1.2	0.389(2)	6.00	38.67(7)	0.2724				0.408(3)
2	0.454(6)	6.00	39.0(1)	0.2901				0.377(6)
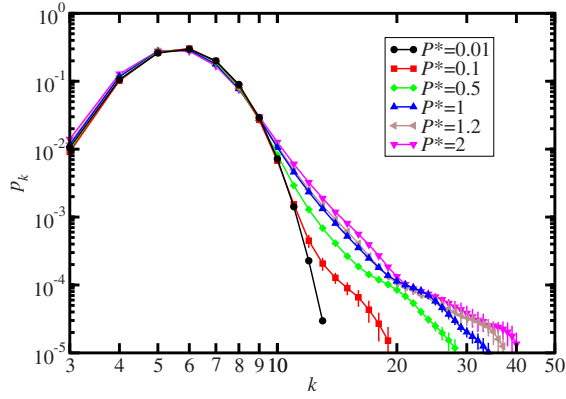
FIG. 4. (Color online) Near-neighbor distribution functions p_k at reduced pressures in the range $0.01 \leq P^* \leq 2$.

which serves to reduce statistical errors. We report the resulting MLE exponents in Table I; the values are slightly smaller than, but generally consistent with, those obtained from least-squares fitting.

Interestingly, γ is relatively insensitive to the packing fraction, being in the region 5–6; the uncertainties quoted in Table I are associated with the fitting procedure, and so they are underestimates. Naively, if the number of neighbors is proportional to the disk diameter, then one might expect $p_k \sim k^{-4}$; in reality, γ is significantly greater than 4. The apparent exponent $\gamma > \alpha$ can be understood by comparing the MC simulation results with the predictions from the ME theory derived in Sec. II C. Figure 6 shows p_k from simulations with $P^* = 0.5$ and $P^* = 1$, along with plots of Eq. (27) computed using the best-fit parameters $a_1 = 5.50$ and $a_1 = 5.39$, respectively, and values of $\langle k^2 \rangle$ reported in Table I. The ME results are in quite good agreement with those from simulations, although the kink at $p_k \sim 10^{-4}$ is not captured so well. But the main points are that in the region of $k = 20$–30, where the simulation results are consistent with a power-law decay, the ME predictions have apparent exponents greater than 4 (at $k = 20$, $\gamma = -d \ln p_k / d \ln k \simeq 5.8$) and that, as $k \to \infty$, p_k approaches the anticipated k^{-4} behavior (at $k = 100$, $\gamma \simeq 4.3$). Of course, this is largely a consequence of
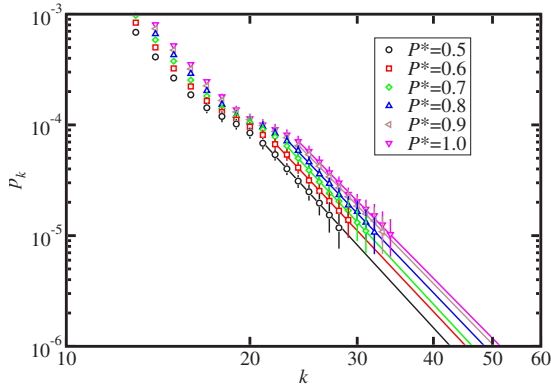

FIG. 5. (Color online) Tails of the near-neighbor distribution functions p_k at reduced pressures in the range $0.5 \leq P^* \leq 1$. The lines are fitted power-law extrapolations $p_k \sim k^{-\gamma}$; the least-squares exponents are reported in Table I.
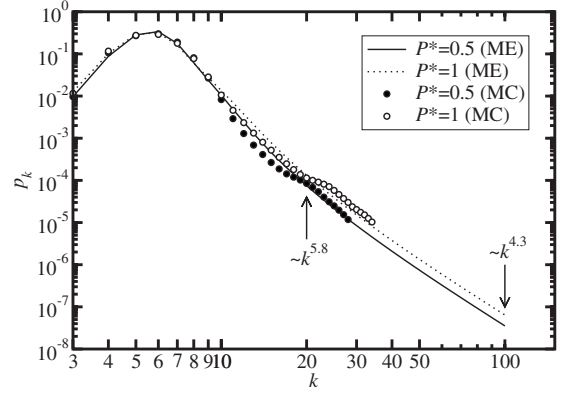

FIG. 6. Near-neighbor distribution functions p_k at reduced pressures of $P^* = 0.5$ (solid points and solid line) and $P^* = 1$ (open points and dotted line) from MC simulation (points) and the ME theory (lines).

the prescription for $K_1(\sigma)$. But the agreement between simulation and theory at moderate k suggests that, at large enough k, the simulated network degree distribution would follow the power law $p_k \sim k^{-4}$.

C. Assortativity

The assortativity of a network, as defined by Newman [18], reflects the tendency of vertices with equal degrees to cluster. A convenient measure of assortativity is clearly defined in Ref. [18], but for clarity the derivation is reproduced here. The degree distribution of vertices attached to randomly selected edges is not equal to p_k, because high-degree vertices have more links. Instead, the distribution is proportional to kp_k and the distribution of the remaining vertices (not including that attached to the randomly selected edge) is $q_k \propto (k+1)p_{k+1}$. The assortativity can then be related to the joint probability distribution function of there being j and k remaining vertices at each end of the selected edge [17]. Denoting this function by e_{jk}, the following properties are to be noted: for an undirected graph $e_{jk} = e_{kj}$, $\Sigma_{jk} e_{jk} = 1$, and $\Sigma_j e_{jk} = q_k$. For networks which are neither assortative nor disassortative, the degrees of the vertices at the ends of the edge are uncorrelated and so $e_{jk} = q_j q_k$. A correlation function between degrees can therefore be defined as $\langle jk \rangle - \langle j \rangle \langle k \rangle = \Sigma_{jk} jk(e_{jk} - q_j q_k)$ where the angular brackets denote an average over all edges in the graph. For the comparison of diverse graphs, it is convenient to normalize this correlation function by its maximal value, which corresponds to the case of a perfectly assortative network, i.e., the degrees of connected vertices are identical. In this case $e_{jk} = q_k \delta_{jk}$ and $\Sigma_{jk} jk(e_{jk} - q_j q_k)$ is equal to the variance σ_q^2 of k according to the distribution q_k. Finally, then, the measure of assortativity is defined as

$$r = \frac{\sum_{jk} jk(e_{jk} - q_j q_k)}{\sigma_q^2}, \tag{28}$$

where r ranges from -1 for a perfectly disassortative network through 0 for a network with no disassortative or as-

sortative mixing (such as a random network [1,18]) to +1 for a perfectly assortative network. The average values of r obtained for the hard-disk neighbor networks are reported in Table I. The results indicate that the hard-disk fluid is strongly assortative at all pressures considered. If the degree of a disk is dictated by its diameter, then in physical terms, the results indicate that "small" disks are preferentially solvated by other small "disks"; the "large" disks—with high degree—are more likely to be solvated by small disks, due to the form of the diameter distribution. Nonetheless, some weak clustering of large disks is apparent in Fig. 3, particularly in Figs. 3(b) and 3(c); note the associations between different "sparse" regions of the network. The physical driving force for the clustering of large disks might be identified with a depletion interaction [51–53] mediated by the osmotic pressure of the small disks, but of course what constitutes the boundary between large and small is not well defined. r decreases slowly and monotonically with increasing packing fraction. One possibility is that as the packing fraction is increased, particle packing and correlations become more pronounced, and the large disks develop links with an increasing number of neighboring small disks, and the assortativity decreases. This process is, of course, accompanied by a broadening of the degree distribution, as illustrated in Fig. 4 and as quantified by the relative width $w=\sqrt{\langle k^2\rangle/\langle k\rangle^2-1}$, reported in Table I. The broadening of p_k and the resulting effects on q_k are already taken into account in the definition of r [Eq. (28)].

The assortativities of real networks vary widely. Most "social" networks, such as scientific co-authorships and movie-actor collaborations, are clearly assortative, with r values up to about 0.4 [18]; successful individuals are often attracted to others. On the other hand, the networks represented by the World Wide Web, the Internet, and most significantly, many biological situations are disassortative (with r values down to about −0.3) [18]; this property may make the network more resilient to random attack, since the hubs (which may play crucial roles in the function of the network) are not connected [8]. The present simulation results indicate that if scale-free neighbor networks do exist in the polydisperse hard-disk fluid at pressures in the range $0.5\le P^*\le1$, then they are strongly assortative, with values of r comparable to those found in social networks. It is tempting to speculate that the analogues of groups and communities in social networks [20] are "clusters" of small and large disks in the polydisperse fluid.

IV. CONCLUSIONS

An attempt has been made to realize a scale-free near-neighbor network in computer simulations of a polydisperse fluid of hard disks. Each disk represents a vertex on a graph, and the edges of the graph correspond to links between neighboring disks as identified by a radical tessellation. Working on the naive assumption that the number of links is proportional to the disk diameter, an asymptotic power-law diameter distribution was expected to give an asymptotic power-law degree distribution. The simulation results are consistent with power-law decay—within the limits imposed

by the simulated diameter distribution—but only for a specific range of disk densities in which particle correlations are sufficiently pronounced. The apparent exponent of the degree distribution γ was found to depend weakly on the disk density and to differ from the exponent of the diameter distribution α. A comparison with predictions from a maximum-entropy theory suggests that this decay is not the asymptotic one and that for sufficiently large particles (not accessible in simulations) γ would approach α. The results therefore suggest that, in principle, the near-neighbor network in the polydisperse hard-disk fluid may be scale free. It is anticipated that a similar situation would be obtained with different choices of α, but of course α should be as small as possible if a sufficient number of hubs are to be found in a network of finite size. Earlier results [29] and the form of the maximum-entropy theory suggest that non-power-law diameter distributions will not give rise to a scale-free neighbor network. The assortativity of the network was found to be positive over the whole range of disk densities, reflecting a preference for links between vertices of equal degree. In other words, "small" particles, are preferentially solvated by other small particles and "large" particles show some tendency to cluster together. Finally, some effort was directed toward analyzing the thermodynamic properties of the fluid. No evidence for crystallization at high packing fractions was found. A simple equation of state—derived from a scaled-particle theory—was demonstrated to be accurate up to moderate packing fractions.

In stochastic models of networks, the position of a vertex on a graph does not influence its degree (i.e., the number of other vertices with which it shares edges). But in the case of hard disks at equilibrium, the degree of a disk is dictated by its size and the sizes of its immediate neighbors, through packing constraints. The spatial correlations in fluids, and therefore the properties of the neighbor network, are dictated by the requirement to minimize the free energy of the system. Hence, the apparent scale-free properties of the network are static and do not arise from any dynamic mechanism, such as preferential attachment. It would be interesting to find out whether the formation of assortative, scale-free networks in other contexts can be rationalized using equilibrium statistical mechanics.

An experimental realization of a polydisperse "fluid" could actually be a granular material, with a scale-free size distribution achieved by milling and grinding. Alternatively, by analogy with cellular networks, froths and foams produced with an element of bubble division and disappearance may exhibit a scale-free degree distribution [15,16]. It should be pointed out, however, that in conventional colloidal fluids, polydispersity is usually better described by log-normal or Γ distributions. The physical properties of two-dimensional materials possessing scale-free networks may be of interest and demand further study.

[1] P. Erdös and A. Rényi, Publ. Math. (Debrecen) **6**, 290 (1959).

[2] R. Albert and A.-L. Barabási, Rev. Mod. Phys. **74**, 47 (2002).

[3] R. Albert, H. Jeong, and A.-L. Barabási, Nature (London) **401**, 130 (1999).

[4] A.-L. Barabási, R. Albert, and H. Jeong, Physica A **281**, 69 (2000).

[5] M. Faloutsos, P. Faloutsos, and C. Faloutsos, Comput. Commun. Rev. **29**, 251 (1999).

[6] H. Jeong, B. Tombor, R. Albert, Z. N. Oltvai, and A.-L. Barabási, Nature (London) **407**, 651 (2000).

[7] P. Uetz *et al.*, Nature (London) **403**, 623 (2000).

[8] H. Jeong, S. P. Mason, A.-L. Barabási, and Z. N. Oltvai, Nature (London) **411**, 41 (2001).

[9] F. Liljeros, C. R. Edling, L. A. N. Amaral, H. E. Stanley, and Y. Aberg, Nature (London) **411**, 907 (2001).

[10] M. E. J. Newman, Proc. Natl. Acad. Sci. U.S.A. **98**, 404 (2001).

[11] A.-L. Barabási and R. Albert, Science **286**, 509 (1999).

[12] R. N. Onody and P. A. de Castro, Phys. Rev. E **70**, 037103 (2004).

[13] A.-L. Barabási and E. Bonabeau, Sci. Am. **288**, 50 (2003).

[14] L. Li, D. Alderson, J. C. Doyle, and W. Willinger, Internet Math. **2**, 431 (2006).

[15] R. Delannay and G. Le Caër, Phys. Rev. Lett. **73**, 1553 (1994).

[16] M. F. Miri and N. Rivier, Phys. Rev. E **73**, 031101 (2006).

[17] D. S. Callaway, J. E. Hopcroft, J. M. Kleinberg, M. E. J. Newman, and S. H. Strogatz, Phys. Rev. E **64**, 041902 (2001).

[18] M. E. J. Newman, Phys. Rev. Lett. **89**, 208701 (2002).

[19] M. E. J. Newman, SIAM Rev. **45**, 167 (2003).

[20] M. E. J. Newman and J. Park, Phys. Rev. E **68**, 036122 (2003).

[21] J. S. Andrade, Jr., H. J. Herrmann, R. F. S. Andrade, and L. R. da Silva, Phys. Rev. Lett. **94**, 018702 (2005).

[22] P. B. Thomas and D. Dhar, J. Phys. A **27**, 2257 (1994).

[23] H. D. Rozenfeld and D. ben-Avraham, Phys. Rev. E **75**, 061102 (2007).

[24] J. P. K. Doye and C. P. Massen, Phys. Rev. E **71**, 016128 (2005).

[25] C. P. Massen and J. P. K. Doye, Phys. Rev. E **71**, 046101 (2005).

[26] J. P. K. Doye and C. P. Massen, J. Chem. Phys. **122**, 084105 (2005).

[27] C. P. Massen and J. P. K. Doye, Phys. Rev. E **75**, 037101 (2007).

[28] B. J. Gellatly and J. L. Finney, J. Non-Cryst. Solids **50**, 313 (1982).

[29] C. Annic, J. P. Troadec, A. Gervois, J. Lemaitre, M. Ammi, and L. Oger, J. Phys. I **4**, 115 (1994).

[30] J. P. Troadec, A. Gervois, C. Annic, and J. Lemaitre, J. Phys. I **4**, 1121 (1994).

[31] A. Gervois, C. Annic, J. Lemaitre, M. Ammi, L. Oger, and J. P. Troadec, Physica A **218**, 403 (1995).

[32] D. A. Aboav, Metallography **3**, 383 (1970).

[33] D. Weaire, Metallography **7**, 157 (1974).

[34] D. A. Aboav, Metallography **13**, 43 (1980).

[35] M. A. Peshkin, K. J. Strandburg, and N. Rivier, Phys. Rev. Lett. **67**, 1803 (1991).

[36] N. Rivier, J. Phys. I **4**, 127 (1994).

[37] R. P. Sear and J. A. Cuesta, Phys. Rev. Lett. **91**, 245701 (2003).

[38] H. Reiss, H. L. Frisch, and J. L. Lebowitz, J. Chem. Phys. **31**, 369 (1959).

[39] M. P. Allen and D. J. Tildesley, *Computer Simulation of Liquids* (Clarendon Press, Oxford, 1987).

[40] C. Dress and W. Krauth, J. Phys. A **28**, L597 (1995).

[41] J. W. Liu and E. Luijten, Phys. Rev. Lett. **92**, 035504 (2004).

[42] B. Widom, J. Chem. Phys. **39**, 2808 (1963).

[43] W. R. Smith and S. Labík, Mol. Phys. **80**, 1561 (1993).

[44] S. Labík and W. R. Smith, Mol. Simul. **12**, 23 (1994).

[45] M. P. Allen, G. T. Evans, D. Frenkel, and B. M. Mulder, Adv. Chem. Phys. **86**, 1 (1993).

[46] J.-P. Hansen and I. R. McDonald, *Theory of Simple Liquids* (Academic Press, London, 1986).

[47] P. Calka, Adv. Appl. Probab. **35**, 863 (2003).

[48] V. S. Kumar and V. Kumaran, J. Chem. Phys. **123**, 074502 (2005).

[49] H. Bauke, Eur. Phys. J. B **58**, 167 (2007).

[50] A. Clauset, C. R. Shalizi, and M. E. J. Newman, e-print arXiv:0706.1062.

[51] S. Asakura and F. Oosawa, J. Chem. Phys. **22**, 1255 (1954).

[52] A. Vrij, Pure Appl. Chem. **48**, 471 (1976).

[53] H. N. W. Lekkerkerker, W. C.-K. Poon, P. N. Pusey, A. Stroobants, and P. B. Warren, Europhys. Lett. **20**, 559 (1992).